Optical Transistor for Amplification of Radiation in a Broadband Terahertz Domain

K. H. A. Villegas,[1] F. V. Kusmartsev,[2,3,*] Y. Luo,[2,†] and I. G. Savenko[1,4]
[1]Center for Theoretical Physics of Complex Systems, Institute for Basic Science (IBS), Daejeon 34126, Korea
[2]Micro/Nano Fabrication Laboratory (MNFL), Microsystem and Terahertz Research Center, Chengdu, China
[3]Physics Department, Loughborough University, Loughborough LE11 3TU, United Kingdom
[4]A. V. Rzhanov Institute of Semiconductor Physics, Siberian Branch of Russian Academy of Sciences, Novosibirsk 630090, Russia

(Received 30 December 2018; revised manuscript received 13 October 2019; accepted 23 January 2020; published 26 February 2020)

We propose a new type of optical transistor for a broadband amplification of terahertz radiation. It is made of a graphene-superconductor hybrid, where electrons and Cooper pairs couple by Coulomb forces. The transistor operates via the propagation of surface plasmons in both layers, and the origin of amplification is the quantum capacitance of graphene. It leads to terahertz waves amplification, the negative power absorption, and as a result, the system yields positive gain, and the hybrid acts like an optical transistor, operating with the terahertz light. It can, in principle, amplify even a whole spectrum of chaotic signals (or noise), which is required for numerous biological applications.

DOI: 10.1103/PhysRevLett.124.087701

The growing interest in the terahertz frequency range (0.3–30 THz) is due to its potential applications in diverse fields such as nondestructive probing in medicine, allowing for noninvasive tumor detection, biosecurity, ultrahigh-bandwidth wireless communication networks, vehicle control, atmospheric pollution monitoring, intersatellite communication, and spectroscopy [1–4]. However, the terahertz range still remains a challenge for modern technology due to the lack of a compact, powerful, and scalable solid-state source [5]. This problem is known as the "terahertz gap."

To "close" this gap from the lower frequencies, one can mention electronic devices with negative differential resistance (NDR). For instance, superlattice electronic devices generate higher harmonics by means of NDR [6] and can reach a 0.5 THz gap, while the output power is less than 0.5 mW [7]. The radiation power of resonant tunneling diodes (RTDs) [8] is less than 1 μW, and it further decreases by 3 orders of magnitude at room temperature. Also, RTDs suffer from their small electron transition times and parasitic capacitance, associated with the double-barrier structure.

The use of layered high-temperature superconductors (HTSCs) with intrinsic Josephson junctions, such as $Bi_2Sr_2CaCu_2O_8$ (bismuth strontium calcium copper oxide) [9–11] can produce radiation with Josephson oscillations generated by an applied bias voltage [12,13]. Here, a tunable emission, from 1 to 11 THz, has been recently observed [14]. However, the power output is 1 μW, which is still inadequate for practical applications.

It can be enhanced with the use of Bose-Einstein condensates [15,16]. However, such approach requires a hybridization of several bands with different parity, making the output power small. Quantum cascade lasers (QCLs) [17–19] can generate a high-frequency terahertz radiation, while transistors [20–23], Gunn diodes [24], and frequency multipliers [25] are approaching the terahertz gap from the low-frequency side. The latter covers the whole terahertz range, while having small power. The general fundamental obstacle of all these terahertz sources is the small emission rate (on the order of 10 ms). It can be increased with the Purcell effect when terahertz sources are placed in a cavity [26,27], however, the quantum efficiency is still about 1%, and their manufacture is difficult.

Graphene and carbon nanotubes may serve as highly tunable sources and detectors of terahertz radiation [28–34], and even in terahertz lasers [35–41]. In the dual-gate graphene-channel field-effect transistor [42] embedded into a cavity resonator [43,44], one observes spontaneous broadband light emission in the 0.1–7.6 THz range with the maximum radiation power of $\sim$10 μW at a temperature of 100 K. There are also emerging sources of multiple harmonic generation of terahertz radiation in superlattices [45,46], frequency difference generation in midinfrared QCLs [47], and terahertz optical combs [48].

Graphene covered with a thin film of colloidal quantum dots has a strong photoelectric effect, which provides enormous gain for the photodetection (about 10^8 electrons per photon) [49]; graphene grown on SiC has a strong photoresponse [50], and graphene composites can improve solar cells efficiency [51]. Note, both graphene and the superconductor alone are practically insensitive to light [52]. Here, we show that graphene placed in the vicinity of a superconductor represents an active media with strong light-matter coupling. It can operate as an optical transistor that amplifies broadband electromagnetic radiation. That is useful for studying chemical and biological processes or in telecommunications for encryption-decryption procedures, where it is important to image a whole spectrum.

We consider a system consisting of parallel layers of graphene and superconductor, exposed to an electromagnetic (EM) field incident with the angle θ and linearly

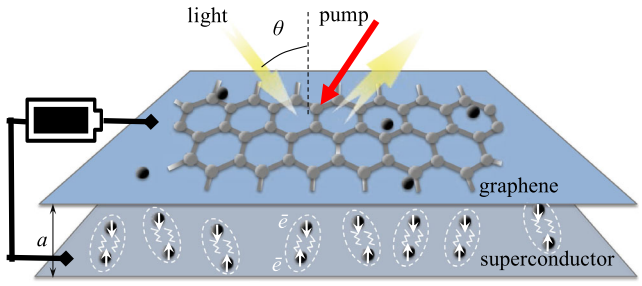

FIG. 1. System schematic. Graphene coupled with a two-dimensional superconductor by the Coulomb force and connected to an electrical pump source (a battery). Figure also shows the pump-probe configuration for the terahertz radiation amplification: The hybrid system is exposed to an external laser (*pump*, depicted by red arrow) and broadband EM field at incidence angle θ (*probe*, depicted by yellow arrows). The frequency of the pump (probe) should be above (below) the superconducting gap. Both the optical and electrical pump can provide energy for the amplification.

polarized along the x-z plane (p polarization), $\mathbf{E}(\mathbf{r},t) = (\sin\theta, \mathbf{0}, \cos\theta)E_0 e^{-i(k_\perp z + \mathbf{k}_\parallel \cdot \mathbf{r} + \omega t)}$, where $\mathbf{k}_\parallel$, ω, and $\mathbf{r}$ are the in-plane wave vector of the field, frequency, and coordinate, respectively (see Fig. 1). Between the graphene layer and superconductor there is a gate voltage that controls its chemical potential. The energy is supplied by ac bias and/or by an external laser (pump) with frequency exceeding the superconducting gap Δ (see Fig. 1). There, exciting quasiparticles in the superconductor are creating NDR.

The electrons in graphene are coupled by the Coulomb interaction, which has the Fourier image given by $v_k = 2\pi e^2/k$, where $\mathbf{k}$ is in-plane momentum (lying in the x-y plane). The electrons between the two layers are also Coulomb coupled, and the Fourier image of the interlayer interaction reads $u_k = 2\pi e^2 \exp(-ak)/k$, where $a = 10$ nm is the separation between the layers.

Using the linear response theory for hybrid systems [53,54], we can write the electron density fluctuations in the graphene layer $\delta n_{k\omega}$ and Cooper pair density fluctuations in the superconducting layer $\delta N_{k\omega}$ as [55]

$$\begin{aligned} \delta n_{k\omega} &= \Pi_{k\omega}(v_k \delta n_{k\omega} + u_k \delta N_{k\omega} + W_{k\omega}), \\ \delta N_{k\omega} &= P_{k\omega}(v_k \delta N_{k\omega} + u_k \delta n_{k\omega} + W_{k\omega}), \end{aligned} \tag{1}$$

where $\Pi_{k\omega} = \Pi^R_{k\omega} + i\Pi^I_{k\omega}$ and $P_{k\omega} = P^R_{k\omega} + iP^I_{k\omega}$ are the complex-valued polarization operators of the graphene and superconductor, respectively, and $W_{k\omega} = eE_0/ik$ is the Fourier image of the potential energy due to the external electric field. From Eqs. (1) we can find the density fluctuations in the graphene $n_{k\omega}$ and in the superconductor $N_{k\omega}$ as linear functions of applied electric field amplitude E_0 (see Supplemental Material [56] for details). Collective plasmonic hybrid modes in the graphene and superconductor can be found from the same system of equations, taking into account the expressions for the polarization loops of the superconductor [55] and graphene [63,64]. Substituting the expressions for $n_{k\omega}$ and $N_{k\omega}$ into the continuity equations, $kj_{k\omega} = -e\omega\delta n_{k\omega}$ and $kJ_{k\omega} = -2e\omega\delta N_{k\omega}$, for graphene and superconductor, respectively, we can determine the electric currents in each of the layers and their impedances Z_G and Z_{SC}. The collective modes of the hybrid system are presented in Fig. 2(a) for the undoped and doped graphene cases. The upper mode has a gap $2\Delta = 2$ meV. If in this hybrid a single graphene layer is not interacting with a superconductor, only one mode exists, which is due to the superconductor.

The formula for the power absorption or gain reads [65]

$$P(\omega) = \frac{1}{2}\left\langle \mathcal{R}e\left[\int d^2 r \mathbf{J}(\mathbf{r},t)\cdot\mathbf{E}^*(\mathbf{r},t)\right]\right\rangle, \tag{2}$$

where the integration is over the graphene plane, and $\langle\cdots\rangle$ denotes time averaging. We normalize the power with the sample area $\int d^2 = l^2$ and the square of the field amplitude E_0^2 to get

$$\mathcal{P}(\omega) = \frac{P(\omega)}{l^2 E_0^2} = \frac{1}{2}\frac{e\omega}{kE_0}\mathcal{R}e[\delta n_{k\omega}]. \tag{3}$$

Figure 2(b) shows the dependence of the power absorption on the EM field incidence angle θ calculated with (3), fixing $\mu = 0$ at the Dirac point by gate voltage. All the curves exhibit critical angles at which the power absorption becomes negative, $\alpha < 0$. This suggests that the incident angle can be used to switch the amplifier device on or off. Furthermore, increasing the frequency of the incident EM wave increases the critical angle.

Figure 2(c) shows the power absorption spectrum. We see that coupling graphene to the superconductor layer results in a negative power absorption in the terahertz frequency range (solid curves and shaded regions). There is no negative absorption region for isolated graphene, where the power absorption remains positive for any frequency ν (dashed curves). When the light incidence angle θ increases, both the maximal intensity (slightly) and the frequency range of the negative light absorption increase [see the shaded area in Figs. 2(b) and 2(c)]. Thus, the angle of light incidence allows us to control the range of light frequencies with the negative absorption.

To understand the θ dependence, note that the wave vector of the plasma wave is related to the projection of the incident light wave vector on the plane of the sample. Both the angular dependence of the absorption and gain are related to the amplitude of this wave propagating on the surface. The light incident perpendicular to the graphene surface cannot excite such plasma waves and, therefore, in this case, we do not have the gain. However, at large incident angle, there is a reflection of the incident radiation

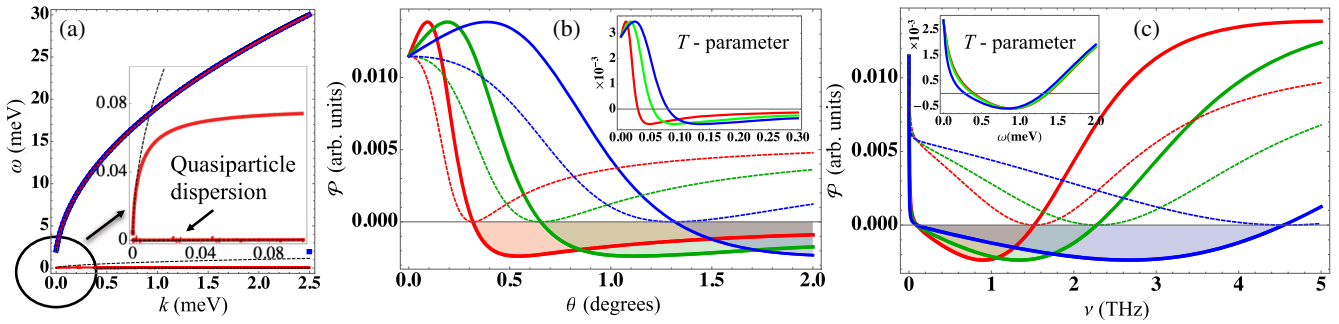

FIG. 2. (a) Hybrid collective plasmonic modes for undoped (blue curves) and doped (red curves, $\mu = 3.0$ meV) graphene layer. Black dashed curves show the modes of isolated doped graphene layer. (Inset) Enlargement of the lower energy modes. (b) Power absorption as a function of the angle of incidence θ (see also Fig. 1) for graphene-superconductor hybrid for frequencies $\nu = 0.5$ (red), 1.0 (green), and 2.0 THz (blue). (c) Graphene power absorption spectrum for the angles of incidence $\theta = 1.0°$ (red), $\theta = 1.5°$ (green), and $\theta = 3.0°$ (blue). Dashed curves show the data corresponding to the isolated graphene. In (b) and (c) $\mu = 0$. (Insets) The effect of temperature $T = 0$ (red), $T = 0.5T_c$ (green), and $T = T_c$ (blue) is shown. The graphene-superconductor separation is $a = 10$ nm.

due to the difference in the refractive index of the hybrid and air. Thus, we conclude that the most optimal effect will be observed at small but nonzero θ. If the system is embedded into a cavity resonator, there might even arise lasing similar to one observed in plasmonic lattices [66,67] or semiconductor superlattices [44].

The mechanism of gain here is similar to one in a waveguide coupled with a superconducting Josephson junction [68]. Then, the optical reflectivity of the system reads $\Gamma = (Z_G - Z_{SC})^2/(Z_G + Z_{SC})^2$. Near the frequency of the plasmon resonance, there is an area of negative differential resistance of the superconductor, $R_{SC} < 0$. If we assume $X_G = 0$ and $X_{SC} = 0$ [68,69], we find $\Gamma > 1$. Note that a graphene transistor [70] can also have NDR (see Sec. III of [56] and [71–73]).

The graphene-superconductor junction (Fig. 1) has a large tunneling resistance. An electron in graphene with energy below the superconducting gap can tunnel into the superconductor only due to the Andreev scattering [74]. The probability of such tunneling is small, since all electrons are paired. Therefore, the resistance of the junction is high. With applied bias voltage above the gap, quasiparticles appear and they can tunnel. As a result, the resistance decreases and NDR arises. The latter can appear even at zero bias when we pump the superconductor with external light with the frequency above the gap. The light excites electron and hole quasiparticles coexisting with superconducting fluctuations on the surface of the superconductor [75]. Then, in addition to the Andreev scattering, there starts normal tunneling of quasiparticles into the superconductor. The resistance of the junction decreases and the NDR arises. Such a mechanism of NDR can exist only in a highly nonequilibrium excited state created by the pump [76].

Graphene separated by a dielectric layer (e.g., made of BN, SiO_2, or Ta_2O_5) from the superconductor (Nb, Pb, or HTSCs) together form a parallel plate capacitor, in which the capacitance C is given by $C = C_{\text{plate}} + C_q$, where C_{plate} is the classical capacitance $C_{\text{plate}} = \epsilon_0 A/a$, A is the area of the sample, and ϵ_o is the dielectric constant (e.g., $\epsilon_o = 3.9$ for SiO_2). The quantum capacitance C_q of graphene emerges due to its conical energy-momentum relation, and it has the form $C_q = 2Ae^2|E_F|/\pi\hbar^2 v_F^2$ [77–79]. The component of incident light parallel to the superconducting surface induces the fluctuation of charge density δn_s, which is associated with a traveling plasmon wave with the amplitude $E_s \sim \delta n_s$, where $\delta n_s = \delta n_{s0}\cos(kx + \omega t)$ (Fig. 3). This charge density wave (CDW) on the surface of the superconductor generates a mirror CDW of the opposite sign in the neutral graphene layer, being of the same order as the charge fluctuations in the superconducting layer, i.e., $\delta n_G \sim \delta n_s$. These plasmons have a

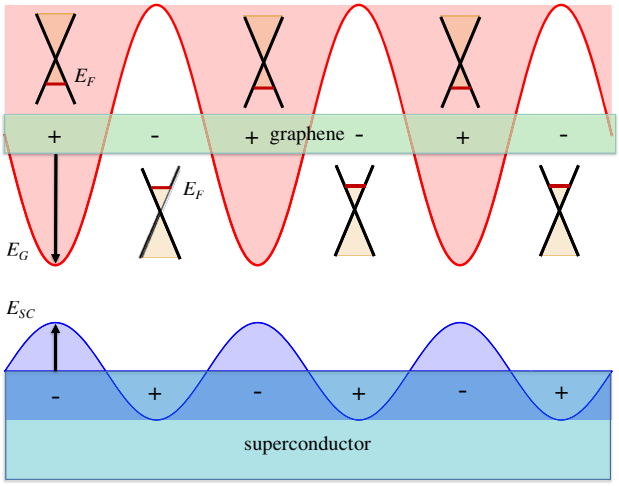

FIG. 3. Schematic of the mechanism of terahertz amplification. The incident light induces a collective hybrid plasmon mode. The interplay between this mode and the quantum capacitance of graphene amplifies the incident electromagnetic field (see text for details).

wavelength larger than a micrometer, and therefore the charge density for each half wavelength can be viewed as a local temporary graphene doping, moving with the wave. During this half period, the charge fluctuation corresponds to the local change in the chemical potential or the Fermi energy E_F, which is directly related to the amplitude of the plasmon wave propagating in graphene E_G. Because of the quantum capacitance of graphene, described by the relation $E_F \sim \sqrt{n_G}$, the waves amplitude $E_G \sim E_F$ is significantly enhanced, and it is different from the amplitude of the plasmon wave, propagating on the surface of the superconductor.

In order to stimulate radiation of electromagnetic waves in the terahertz range (similar to photoconductive antennas [80]), one has to add a supply of energy. It can be done by introducing a pump-probe setup, where the energy required for the amplification of the probe comes from the pump. For the pump, we have to expose graphene to an external laser with the frequency above the superconducting gap. Or we can apply ac bias voltage with the amplitude larger than the gap. Because of the pump, there forms a state, in which energy is accumulated in electronic excitations. To have the pump-probe configuration, we expose the junction to an additional external light (probe) with the frequency lower than the gap. Then, there on the surface will emerge superconducting charge density fluctuations. Effectively, they represent coherent waves traveling inside the capacitor formed by the graphene and superconductor. Because of graphene quantum capacitance [77–79], the amplitude of these electromagnetic waves is amplified. The energy is provided by the pump, resulting in negative light absorption for a probe (see Fig. 2) or a reflection coefficient larger than 1.

Note that the graphene-superconductor system possesses many benefits. Both superconducting and graphene layers have giant mobility and small resistivity, giving rise to minute losses. With increasing temperature, the superconducting gap decreases, while graphene mobility changes a little [81,82]. Since the radiation amplification occurs in graphene, the temperature has a weak effect on the operation of the terahertz transistor [see insets in Figs. 2(b) and 2(c)]. The working temperature range is similar to one for the stack of the Josephson junctions made of HTSCs [9,10], and it is limited by the critical temperature T_c.

The radiation power reads $P_r = \langle V_g I \rangle$, where the voltage V_g and the transverse current I are periodically changing in time around the Dirac point [83]. Then, assuming simple periodic behavior for both $I(t)$ and $V_g(t)$ and the graphene-superconductor separation $a = 10$ nm [84], the maximal outcome power reads $\langle I \times V_g \rangle \sim 200$–$250\ \mu\mathrm{W/cm}^2$ [85]. Evidently, it can be increased for larger areas of the surface or employing multilayer hybrid structures.

Conclusions.—We have shown that, in a hybrid graphene-superconductor system exposed to an electromagnetic field of light, the absorption coefficient can become negative in a certain range of frequencies and at a nonzero angle of incidence. We suggest that the system can serve as an amplifier of terahertz radiation. The essence of the amplification is the quantum capacitance of graphene, which provides the conversion of the charge density wave induced by incident light into emitted radiation with much stronger intensity. That is also related to the negative differential conductivity of the hybrid, where there is a strong Coulomb coupling of graphene and superconductor.

Such devices are now in strong demand and may be complementary to quantum cascade lasers. Moreover, the use of high-temperature superconductors extends the range of temperatures required for their operation. The existence of Dirac or Weyl cones in graphene, topological insulators, and Weyl semimetals brings in a new physical concept called quantum capacitance. Its essence is in strong dependence of the Fermi energy on the charge doping. A weak charge density wave can induce a strong electric field, allowing us to achieve the amplification of incident electromagnetic radiation.

The situation is somewhat similar to lasers, where the pumping results in the population inversion. The difference is that, here, the amplification can occur in a broad frequency range simultaneously, while in lasers it is pinned to a specific resonant frequency. Such amplification of the broadband spectrum, e.g., for chaotic or noise radiation, opens exciting opportunities of new types of molecular and biological noise spectroscopy, where the response of the system can be measured in a broad frequency range, providing new opportunities in molecular and biological noise spectroscopy [86–88].

We thank Vadim Kovalev and Gennadii Sergienko for fruitful discussions. K. H. V. and I. G. S. acknowledge the support of the Institute for Basic Science in Korea (Project No. IBS-R024-D1) and the Russian Foundation for Basic Research (Project No. 18-29-20033).

*Corresponding author.
F.Kusmartsev@lboro.ac.uk
†luoyi@mtrc.ac.cn

[1] F. H. Raab, P. Asbeck, S. Cripps, P. B. Kenington, Z. B. Popovic, N. Pothecary, J. F. Sevic, and N. O. Sokal, Power amplifiers and transmitters for RF and microwave, IEEE Trans. Microwave Theory Tech. **50**, 814 (2002).
[2] J. M. Chamberlain, Where optics meets electronics: Recent progress in decreasing the terahertz gap, Phil. Trans. R. Soc. A **362**, 199 (2004).
[3] H. Eisele, State of the art and future of electronic sources at terahertz frequencies, Electron. Lett. **46**, S8 (2010).
[4] D. M. Mittleman, Twenty years of terahertz imaging, Opt. Express **26**, 9417 (2018).
[5] D. Dragoman and M. Dragoman, Terahertz fields and applications, Prog. Quantum Electron. **28**, 1 (2004).

[6] K. N. Alekseev, E. H. Cannon, F. V. Kusmartsev, and D. K. Campbell, Fractional and unquantized dc voltage generation in THz-driven semiconductor superlattices, Europhys. Lett. **56**, 842 (2001).
[7] H. Eisele, L. Li, and E. H. Linfield, High-performance GaAs/AlAs superlattice electronic devices in oscillators at frequencies 100–320 GHz, Appl. Phys. Lett. **112**, 172103 (2018).
[8] T. Maekawa, H. Kanaya, S. Suzuki, and M. Asada, Oscillation up to 1.92 THz in resonant tunneling diode by reduced conduction loss, Appl. Phys. Express **9**, 024101 (2016).
[9] L. Ozyuzer, A. E. Koshelev, C. Kurter, N. Gopalsami, Q. Li, M. Tachiki, K. Kadowaki, T. Yamamoto, H. Minami, H. Yamaguchi, and T. Tachiki, Emission of coherent THz radiation from superconductors, Science **318**, 1291 (2007).
[10] U. Welp, K. Kadowaki, and R. Kleiner, Superconducting emitters of THz radiation, Nat. Photonics **7**, 702 (2013).
[11] S. Hancong *et al.*, Compact High-Tc Superconducting Terahertz Emitter Operating up to 86 K, Phys. Rev. Appl. **10**, 024041 (2018).
[12] M. Gaifullin *et al.*, Collective Josephson Plasma Resonance in BiSCCO, Phys. Rev. Lett. **75**, 4512 (1995).
[13] M. Gaifullin, Y. Matsuda, N. Chikumoto, J. Shimoyama, and K. Kishio, Abrupt Change of Josephson Plasma Frequency in BiSCCO, Phys. Rev. Lett. **84**, 2945 (2000).
[14] E. A. Borodianskyi and V. M. Krasnov, Josephson emission with frequency span 1–11 THz from small $Bi_2Sr_2CaCu_2O_8$ mesa structures, Nat. Commun. **8**, 1742 (2017).
[15] K. V. Kavokin, M. A. Kaliteevski, R. A. Abram, A. V. Kavokin, and S. Sharkova, Stimulated emission of terahertz radiation by exciton-polariton lasers, Appl. Phys. Lett. **97**, 201111 (2010).
[16] I. G. Savenko, I. A. Shelykh, and M. A. Kaliteevski, Nonlinear Terahertz Emission in Semiconductor Microcavities, Phys. Rev. Lett. **107**, 027401 (2011).
[17] R. Köhler, A. Tredicucci, F. Beltram, H. E. Beere, E. H. Linfield, A. G. Davies, D. A. Ritchie, R. C. Iotti, and F. Rossi, Terahertz semiconductor-heterostructure laser, Nature (London) **417**, 156 (2002).
[18] B. S. Williams, Terahertz quantum-cascade lasers, Nat. Photonics **1**, 517 (2007).
[19] J. Faist, *Quantum Cascade Lasers* (Oxford University Press, Oxford, 2013).
[20] H. W. Hübers, S. G. Pavlov, and V. N. Shastin, Terahertz lasers based on germanium and silicon, Semicond. Sci. Technol. **20**, S211 (2005).
[21] Y. Chassagneux, R. Colombelli, W. Maineult, S. Barbieri, H. E. Beere, D. A. Ritchie, S. P. Khanna, E. H. Linfield, and A. G. Davies, Electrically pumped photonic-crystal terahertz lasers controlled by boundary conditions, Nature (London) **457**, 174 (2009).
[22] J. Lusakowski, W. Knap, N. Dyakonova, L. Varani, J. Mateos, T. Gonzalez, Y. Roelens, S. Bollaert, A. Cappy, and K. Karpierz, Voltage tuneable terahertz emission from a ballistic nanometer InGaAs/InAlAs transistor, J. Appl. Phys. **97**, 064307 (2005).
[23] P. Li, Y. C. Wang, and J. Z. Zhang, All-optical fast random number generator, Opt. Exp. **18**, 20360 (2010).
[24] S. Pérez, T. González, D. Pardo, and J. Mateos, Terahertz Gunn-like oscillations in InGaAs/InAlAs planar diodes, J. Appl. Phys. **103**, 094516 (2008).
[25] A. Maestrini, J. S. Ward, J. J. Gill, C. Lee, B. Thomas, R. h. Lin, G. Chattopadhyay, and I. Mehdi, A frequency-multiplied source with more than 1 mW of power across the 840-900-GHz band, IEEE Trans. Microwave Theory Technol. **58**, 1925 (2010).
[26] Y. Todorov, I. Sagnes, and I. Abram, and C. Minot, Purcell Enhancement of Spontaneous Emission from Quantum Cascades inside Mirror-Grating Metal Cavities at THz Frequencies, Phys. Rev. Lett. **99**, 223603 (2007).
[27] Y. Chassagneux, R. Colombelli, W. Maineult, S. Barbieri, H. E. Beere, D. A. Ritchie, S. P. Khanna, E. H. Linfield, and A. G. Davies, Electrically pumped photonic-crystal terahertz lasers controlled by boundary conditions, Nature (London) **457**, 174 (2009).
[28] M. E. Portnoi, O. V. Kibis, and M. R. da Costa, Terahertz emitters and detectors based on carbon nanotubes, Proc. SPIE Int. Soc. Opt. Eng. **6328**, 632805 (2006).
[29] O. V. Kibis, M. R. da Costa, and M. E. Portnoi, Generation of terahertz radiation by hot electrons in carbon nanotubes, Nano Lett. **7**, 3414 (2007).
[30] M. E. Portnoi, O. V. Kibis, and M. R. Da Costa, Terahertz applications of carbon nanotubes, Superlattices Microstruct. **43**, 399 (2008).
[31] S. A. Mikhailov, Non-linear graphene optics for terahertz applications, Microelectron. J. **40**, 712 (2009).
[32] K. G. Batrakov, O. V. Kibis, P. P. Kuzhir, M. R. Da Costa, and M. E. Portnoi, Terahertz processes in carbon nanotubes, J. Nanophoton. **4**, 041665 (2010).
[33] R. Hartmann, J. Kono, and M. E. Portnoi, Terahertz science and technology of carbon nanomaterials, Nanotechnology **25**, 322001 (2014).
[34] V. Ryzhii, T. Otsuji, M. Ryzhii, V. Ya Aleshkin, A. A. Dubinov, D. Svintsov, V. Mitin, and M. S. Shur, Graphene vertical cascade interband terahertz and infrared photodetectors, 2D Mater. **2**, 025002 (2015).
[35] D. Yadav, S. B. Tombet, T. Watanabe, S. Arnold, V. Ryzhii, and T. Otsuji, Terahertz wave generation and detection in double-graphene layered van der Waals heterostructures, 2D Mater. **3**, 045009 (2016).
[36] A. Satou, T. Otsuji, and V. Ryzhii, Theoretical study of population inversion in graphene under pulse excitation, Jpn. J. Appl. Phys. **50**, 70116 (2011).
[37] A. Satou, V. Ryzhii, Y. Kurita, and T. Otsuji, Threshold of terahertz population inversion and negative dynamic conductivity in graphene under pulse photoexcitation. J. Appl. Phys. **113**, 143108 (2013).
[38] V. Ryzhii, M. Ryzhii, V. Mitin, A. Satou, and T. Otsuji, Effect of heating and cooling of photogenerated electron-hole plasma in optically pumped graphene on population inversion, Jpn. J. Appl. Phys. **50**, 094001 (2011).
[39] T. Otsuji, S. B. Tombet, A. Satou, M. Ryzhii, and V. Ryzhii, Terahertz-wave generation using graphene: Toward new types of terahertz lasers, IEEE J. Sel. Top. Quantum Electron. **19**, 8400209 (2013).
[40] S. Boubanga-Tombet, S. Chan, T. Watanabe, A. Satou, V. Ryzhii, and T. Otsuji, Ultrafast carrier dynamics and

terahertz emission in optically pumped graphene at room temperature, Phys. Rev. B **85**, 035443 (2012).
[41] T. Li, L. Luo, M. Hupalo, J. Zhang, M. C. Tringides, J. Schmalian, and J. Wang, Femtosecond Population Inversion and Stimulated Emission of Dense Dirac Fermions in Graphene, Phys. Rev. Lett. **108**, 167401 (2012).
[42] V. Ryzhii, M. Ryzhii, V. Mitin, and T. Otsuji, Toward the creation of terahertz graphene injection laser, J. Appl. Phys. **110**, 094503 (2011).
[43] Y. Deepika, G. Tamamushi, T. Watanabe *et al.*, Terahertz light-emitting graphene-channel transistor toward single-mode lasing, Nanophotonics **7**, 741 (2018).
[44] A. E. Hramov, V. V. Makarov, A. A. Koronovskii, F. V. Kusmartsev *et al.*, Subterahertz Chaos Generation by Coupling a Superlattice to a Linear Resonator, Phys. Rev. Lett. **112**, 116603 (2014).
[45] M. F. Pereira, J. P. Zubelli, D. Winge, A. Wacker, A. S. Rodrigues, V. Anfertev, and V. Vaks, Theory and measurements of harmonic generation in semiconductor superlattices with applications in the 100 GHz to 1 THz, Phys. Rev. B **96**, 045306 (2017).
[46] A. Apostolakis and M. F. Pereira, Controlling the harmonic conversion efficiency in semiconductor superlattices by interface roughness design, AIP Adv. **9**, 015022 (2019).
[47] M. Razeghi, Q. Y. Lu, N. Bandyopadhyay, W. Zhou, D. Heydari, Y. Bai, and S. Slivken, Quantum cascade lasers: from tool to product, Opt. Express **23**, 8462 (2015).
[48] A. Forrer, M. Rösch, M. Singleton, M Beck, J. Faist, and G. Scalari, Coexisting frequency combs spaced by an octave in a monolithic quantum cascade laser, Opt. Express **26**, 23167 (2018).
[49] G. Konstantatos, M. Badioli, and F. H. L. Koppens, Hybrid graphene-quantum dot phototransistors with ultrahigh gain, Nat. Nanotechnol. **7**, 363 (2012).
[50] A. B. G. Trabelsi, F. V. Kusmartsev, M. B. Gaifullin, A. Kusmartseva, and M. Oueslati, Morphological imperfections of epitaxial graphene: From a hindrance to the generation of new photo-responses in the visible domain, Nanoscale **9**, 11463 (2017).
[51] R. Bkakri, O. E. Kusmartseva, F. V. Kusmartsev, M. Song, and A. Bouazizi, Degree of phase separation effects on the charge transfer properties of P3HT: Graphene nanocomposites, J. Lumin. **161**, 264 (2015).
[52] K. C. Yung, W. M. Wu, M. P. Pierpoint, and F. V. Kusmartsev, Introduction to graphene electronics—a new era of digital transistors and devices, Contemp. Phys. **54**, 233 (2013).
[53] M. V. Boev, V. M. Kovalev, and I. G. Savenko, Magnetoplasmon Fano resonance in Bose-Fermi mixtures, Phys. Rev. B **94**, 241408(R) (2016).
[54] V. M. Kovalev and I. G. Savenko, Paramagnetic resonance in spin-polarized disordered Bose-Einstein condensates, Sci. Rep. **7**, 2076 (2017).
[55] K. H. A. Villegas, V. M. Kovalev, F. V. Kusmartsev, and I. G. Savenko, Shedding light on topological superconductors, Phys. Rev. B **98**, 064502 (2018).
[56] See Supplemental Material at http://link.aps.org/supplemental/10.1103/PhysRevLett.124.087701 for the details of the general theory of the light-matter interaction in a hybrid graphene-superconductor system, including the derivation of the polarization function of the superconductor at finite temperatures and NDR, which includes Refs. [57–62].
[57] A. A. Abrikosov, L. P. Gorkov, and I. E. Dzyaloshinski, *Methods of Quantum Field Theory in Statistical Physics* (Courier Corp., New York, 2012).
[58] A. L. Fetter and J. D. Walecka, *Quantum Theory of Many-Particle Systems* (Dover Publications, New York, 2003).
[59] P. I. Arseev, S. O. Loiko, and N. K. Fedorov, Theory of gauge-invariant response of superconductors to an external electromagnetic field, Phys. Usp. **49**, 1 (2006).
[60] M. Buttiker, Absence of backscattering in the quantum Hall effect in multiprobe conductors, Phys. Rev. B **38**, 9375 (1988).
[61] M. Buttiker, Edge-state physics without magnetic fields, Science **325**, 278 (2009).
[62] A. O'Hare, F. V. Kusmartsev, and K. I. Kugel, A stable flat form of two-dimensional crystals: Could graphene, silicene, germanene be minigap semiconductors? Nano Lett. **12**, 1045 (2012).
[63] B. Wunsch, T. Stauber, F. Sols, and F. Guinea, Dynamical polarization of graphene at finite doping, New J. Phys. **8**, 318 (2006).
[64] E. H. Hwang and S. Das Sarma, Dielectric function, screening, and plasmons in two-dimensional graphene, Phys. Rev. B **75**, 205418 (2007).
[65] L. D. Landau and E. M. Lifshitz, *Electrodynamics of Continuous Media* (Pergamon Press, New York, 1960).
[66] Plasmons can be treated as bosons obeying the Bose-Einstein distribution. However, under external irradiation there can appear a virtual inversion of their population and their continuous stimulated emission (positive gain) accompanied by the amplification of the incident light. In our case, it corresponds to $\alpha < 0$.
[67] W. Zhou, M. Dridi, J. Y. Suh, C. H. Kim, D. T. Co, M. R. Wasielewski, G. C. Schatz, and T. W. Odom, Lasing action in strongly coupled plasmonic nanocavity arrays, Nat. Nanotechnol. **8**, 506 (2013).
[68] N. F. Pedersen and S. Madsen, THz generation using fluxon dynamics in high temperature superconductors, IEEE Trans. Appl. Supercond. **19**, 726 (2009).
[69] Note that here the absorption and gain have been calculated directly as the power of the absorbed or emitted electromagnetic radiation with Eq. (2), on the basis of the solutions of Eq. (1). The concept of impedance has not been used in this calculation. However, from the same equations, one can find impedances of the graphene and superconductor as coefficients proportional to density fluctuations of the graphene and superconductor, or ac electric currents expressed through these density variations, respectively, over E_0. After changing of variables, Eq. (1) can be presented in the form where these impedances are unknown variables. Then the results obtained for the gain by direct calculation of the emitted power can be interpreted with the concept of the graphene and superconductor impedances, characterizing the hybrid system. This argument with impedances for the graphene and superconductor has been used just for clarification of the effect and it provides an alternative interpretation of the gain phenomenon.

[70] L. Britnell, R. V. Gorbachev, A. K. Geim, L. A. Ponomarenko, A. Mishchenko, M. T. Greenaway, T. M. Fromhold, K. S. Novoselov, and L. Eaves, Resonant tunnelling and negative differential conductance in graphene transistors, Nat. Commun. **4**, 1794 (2013).

[71] R. Kummel, U. Gunsenheimer, and R. Nicolsky, Andreev scattering of quasiparticle wave packets and current-voltage characteristics of superconducting metallic weak links, Phys. Rev. B **42**, 3992 (1990).

[72] T. Hyart, K. N. Alekseev, and E. V. Thuneberg, Bloch gain in dc-ac-driven semiconductor superlattices in the absence of electric domains, Phys. Rev. B **77**, 165330 (2008).

[73] T. Hyart, M. Jussi, and K. N. Alekseev, Model of the Influence of an External Magnetic Field on the Gain of Terahertz Radiation from Semiconductor Superlattices, Phys. Rev. Lett. **103**, 117401 (2009).

[74] A. Andreev, The thermal conductivity of the intermediate state in superconductors, Sov. Phys. JETP **19**, 1228 (1964), http://www.jetp.ac.ru/cgi-bin/e/index/e/19/5/p1228?a=list.

[75] L. Aslamazov and A. Larkin, *Effect of Fluctuations on the Properties of a Superconductor above the Critical Temperature*, 30 Years of the Landau Institute—Selected Papers (World Scientific, Singapore, 1996), pp. 23–28.

[76] As in QCLs, scattering and dephasing mechanisms limit the gain bandwidth and can flatten and eliminate the gain [89]. Here the plasmon scattering within each and between two graphene and superconducting layers can not only broaden the width of the optical transition, but can also enable optical gain and absorption to coexist, constituting the Wacker-Pereira mechanism of optical gain [89–91], as observed in QCLs [92,93]. It provides one of the explanations why $\alpha(\omega) = 1 - \Gamma(\omega)$ is negative below the plasmon resonance.

[77] G. L. Yu *et al.*, Interaction phenomena in graphene seen through quantum capacitance, Proc. Natl. Acad. Sci. U.S.A. **110**, 3282 (2013).

[78] A. B. G. Trabelsi, F. V. Kusmartsev, B. J. Robinson, A. Ouerghi, O. E. Kusmartseva, O. V. Kolosov, R. Mazzocco, M. B. Gaifullin, and M. Oueslati, Charged nano-domes and bubbles in epitaxial graphene, Nanotechnology **25**, 165704 (2014).

[79] A. B. G. Trabelsi, F. V. Kusmartsev, D. M. Forrester, O. E. Kusmartseva, M. B. Gaifullin, P. Cropper, and M. Oueslati, The emergence of quantum capacitance in epitaxial graphene, J. Mater. Chem. C **4**, 5829 (2016).

[80] N. M. Burford and M. O. El-Shenawee, Review of terahertz photoconductive antenna technology, Opt. Eng. **56**, 010901 (2017).

[81] F. V. Kusmartsev and A. M. Tsvelik, Semi-metallic properties of a heterojunction, JETP Lett. **42**, 257 (1985), http://www.jetpletters.ac.ru/ps/1421/article_21594.shtml.

[82] F. V. Kusmartsev, W. M. Wu, M. P. Pierpoint, and K. C. Yung, in *Application of Graphene Within Optoelectronic Devices and Transistors*, Applied Spectroscopy and the Science of Nanomaterials (Springer, Singapore, 2015), pp. 191–221.

[83] Note that supporting zero chemical potential we expect to see a nonzero radiation power, which is just an average $V_g(t) \times I(t)$ over the photocurrent period. The output power is maximized when the chemical potential is pinned at the Dirac point, since in this case the voltage variation $V_g(t)$ has a maximal amplitude. On the other hand, if we apply an external ac voltage $V_g(t)$ to the hybrid system, the transistor might radiate terahertz radiation even without external incident light. In this case, the radiation power of the system will be exactly proportional to $P = \langle V_g(t) I(t) \rangle$, where the average is taken over the oscillation period and here a fraction of this energy will be wasted in thermal Joule losses. However, such a source of terahertz radiation requires a special setup for the applied voltage to maximize the effect of quantum capacitance.

[84] In our calculations, we used a relatively large value for the graphene-superconductor separation, $a = 10$ nm, which is several orders of magnitude smaller than the wavelength of terahertz radiation. The smaller the separation, the stronger the effect. However, at very small separation there may arise a proximity effect. That limits the separation distance to a superconducting coherence length, which is for HTSCs about ~1–2 nm.

[85] Such time-dependent periodically changing voltage $V_g(t)$ on graphene is associated with the plasma wave induced in graphene by the incident light. On average, the voltage variation vanishes, $\langle V_g \rangle = 0$, while the radiated power does not, since the current has the same periodic oscillations and the power depends on their product [83]. During the operation of the device, the voltage in graphene can reach 40–50 mV. That limit arises due to electron scattering by optical phonons, which will be generated at higher voltage with account for nonlinear effects [94,95]. The driving photocurrent through 1 cm^2 of graphene is on the order of 10 mA. This value is limited by the Joule heating of the superconductor surface region.

[86] V. P. Koshelets *et al.*, Superconducting integrated terahertz spectrometers, IEEE Trans. Terahertz Sci. Technol. **5**, 687 (2015).

[87] D. R. Gulevich, V. P. Koshelets, and F. V. Kusmartsev, Josephson flux-flow oscillator: The microscopic tunneling approach, Phys. Rev. B **96**, 024515 (2017).

[88] V. A. Yampol'skii, S. Savel'ev, O. V. Usatenko, S. S. Mel'nik, F. V. Kusmartsev, A. A. Krokhin, and F. Nori, Controlled terahertz frequency response and transparency of Josephson chains and superconducting multilayers, Phys. Rev. B **75**, 014527 (2007).

[89] M. F. Pereira, Jr. and S. Tomić, Intersubband gain without global inversion through dilute nitride band engineering, Appl. Phys. Lett. **98**, 061101 (2011).

[90] A. Wacker, in *Quantum Cascade Laser: An Emerging Technology*, Nonlinear Laser Dynamics (John Wiley & Sons, Ltd, Berlin, 2012).

[91] A. Wacker, Lasers: Coexistence of gain and absorption, Nat. Phys. **3**, 298 (2007).

[92] R. Terazzi, T. Gresch, M. Giovannini, N. Hoyler, N. Sekine, and J. Faist, Bloch gain in quantum cascade lasers, Nat. Phys. **3**, 329 (2007).

[93] D. G. Revin, M. R. Soulby, J. W. Cockburn, Q. Yang, C. Manz, and J. Wagner, Dispersive gain and loss in midinfrared quantum cascade laser, Appl. Phys. Lett. **92**, 081110 (2008).

[94] M. M. Glazov and S. D. Ganichev, High frequency electric field induced nonlinear effects in graphene, Phys. Rep. **535**, 101 (2014).

[95] S. D. Ganichev and W. Prettl, *Intense Terahertz Excitation of Semiconductors* (Oxford University Press, Oxford, 2006).